JOURNAL OF VIROLOGY, June 2005, p. 7698–7706 Vol. 79, No. 12
0022-538X/05/$08.00+0 doi:10.1128/JVI.79.12.7698–7706.2005
Copyright © 2005, American Society for Microbiology. All Rights Reserved.

Factors Required for the Uridylylation of the Foot-and-Mouth Disease Virus 3B1, 3B2, and 3B3 Peptides by the RNA-Dependent RNA Polymerase ($3D^{pol}$) In Vitro

Arabinda Nayak,[1] Ian G. Goodfellow,[2] and Graham J. Belsham[1]*

BBSRC Institute for Animal Health, Pirbright, Woking, Surrey GU24 ONF, United Kingdom,[1] and School of Animal and Microbial Sciences, University of Reading, Whiteknights, P.O. Box 228, Reading RG6 6AJ, United Kingdom[2]

Received 18 November 2004/Accepted 10 March 2005

The 5′ terminus of picornavirus genomic RNA is covalently linked to the virus-encoded peptide 3B (VPg). Foot-and-mouth disease virus (FMDV) is unique in encoding and using 3 distinct forms of this peptide. These peptides each act as primers for RNA synthesis by the virus-encoded RNA polymerase $3D^{pol}$. To act as the primer for positive-strand RNA synthesis, the 3B peptides have to be uridylylated to form VPgpU(pU). For certain picornaviruses, it has been shown that this reaction is achieved by the $3D^{pol}$ in the presence of the 3CD precursor plus an internal RNA sequence termed a *c*is-acting *r*eplication *e*lement (*cre*). The FMDV *cre* has been identified previously to be within the 5′ untranslated region, whereas all other picornavirus *cre* structures are within the viral coding region. The requirements for the in vitro uridylylation of each of the FMDV 3B peptides has now been determined, and the role of the FMDV *cre* (also known as the 3*B-u*ridylylation *s*ite, or *bus*) in this reaction has been analyzed. The poly(A) tail does not act as a significant template for FMDV 3B uridylylation.

Picornaviruses, including foot-and-mouth disease virus (FMDV), poliovirus (PV), and human rhinoviruses (HRVs), have a positive-sense RNA genome of about 8 kb that is infectious (1, 5). Following virus attachment and entry into the cell, the RNA genome is delivered into the cytoplasm and translation of the genome is required to produce the viral proteins that are necessary for virus assembly and RNA replication. The genome encodes a single large polyprotein that is processed, largely by internal *trans*-acting proteases, to produce about 12 mature proteins plus various precursors (some of these have distinct functions). The proteins encoded within the P1 region form the capsid, while proteins encoded in the P2 and P3 regions are required for RNA replication. After some rounds of translation, there has to be a switch so that translation of the viral RNA is stopped and RNA replication can commence, since these two processes appear incompatible on the same RNA molecule (11). Most picornaviruses replicate with high efficiency within susceptible cells, and within a few hours, the amount of viral RNA can represent 5% of the total RNA in cells (a level similar to that of all the cellular cytoplasmic mRNAs together). Nearly all of the FMDV RNA generated by replication is infectious; indeed, microinjection of cells with as little as 1 to 2 molecules of viral RNA is sufficient to initiate an infection (4). Thus, the replication of FMDV genomes within cells is remarkably efficient.

To replicate the positive-sense genome, an antisense RNA has to be synthesized which then functions as the template for the production of new positive-sense infectious genomes (32). RNA is synthesized by the viral 3D protein that functions as an RNA-dependent RNA polymerase and will be referred to as $3D^{pol}$. Interestingly, $3D^{pol}$ requires the uridylylated form of the 3B/VPg peptide (VPgpU or VPgpUpU) to act as the primer for both positive- and negative-strand synthesis. In recent years, the mechanism involved in the synthesis of this modified peptide primer has become clearer (32). Evidence has accumulated for the presence of *cis*-acting RNA elements located internally within picornavirus genomes that are required for RNA replication and have been shown to act as the template for the production of the uridylylated peptide primer. Initially, it was found that certain sequences within the P1 coding sequence of HRV type 14 (HRV-14) were required to achieve efficient replication of replicons based on this virus (26). This contrasted with previous studies on PV that had demonstrated that the entire capsid coding sequence could be deleted without affecting RNA replication (19). Further work (27) identified the critical RNA element as a specific stem-loop structure, termed a *cis*-acting replication element (*cre*), located within the 1D (VP1) coding region of the HRV-14 genome. Subsequently, similar *cre* motifs have been identified in other picornavirus genomes (12, 15, 23). Each of the *cre*'s include a conserved sequence motif of AAACA located within a loop at the end of a stable stem structure. These elements (about 50 to 60 nucleotides [nt] in length) occur in different places within the picornavirus genomes; the *cre*'s from HRV-14, HRV-2, cardioviruses, and PV are within the coding regions for 1D, 2A, 1B, and 2C, respectively (12, 15, 23, 27). Furthermore the *cre*'s can be moved without blocking function (15). It has been shown that the PV and HRV-2 *cre* structures act as the template for the uridylylation of VPg (3B) (to produce VPgpU and VPgpUpU) by the 3D RNA polymerase in vitro (12, 34). Evidence has been presented that this process involves a "slide-back" mechanism on the AAACA motif (36). It is noteworthy that, within cell-free replication systems, the PV *cre* is only required for the synthesis of positive-sense RNA strands (17, 28, 29).

Recently, Mason et al. (24) presented evidence for a *cre*

* Corresponding author. Mailing address: BBSRC Institute for Animal Health, Pirbright, Woking, Surrey GU24 ONF, United Kingdom. Phone: 44 (0)1483 232441. Fax: 44 (0)1483 232448. E-mail: graham.belsham@bbsrc.ac.uk.

TABLE 1. Oligonucleotides used in PCR and mutagenesis

Name	Sequence (5′–3′)
3DFORBGL	CCAGATCTGGGTTGATTGTGGACACCAGAGAT
3DREVSPH	CCGCATGCCGCGTCACCGCACACGGCGTTCAC
3CFORBGL	CCAGATCTAGTGGTGCCCCACCGACCGACTTG
C163FOR	CACCAAGGCTGGTTACGGCGGAGGAGCCGTTC
C163REV	GAACGGCTCCTCCGCCGTAACCAGCCTTGGTG
SacIImutFor	CAGGGTAAACGCCGTGGCGCGCTCATCGAC
SacIImutRev	GTCGATGAGCGCGCCACGGCGTTTACCCTG
Ub3DpolSacII	GCGCCGCGGTGGAGGGTTGATTGTGGACACCAGA
Ub3DpolBgIII	GCGAGATCTTTACGCGTCACCGCACACGGCGTT
GC-cremut-FOR(A1-C)	GAGGAGGACTTGTACCAACACGATCTAAACAG
GC-cremut-REV(A1-C)	CTGTTTAGATCGTGTTGGTACAAGTCCTCCTC
GC-cremut-FOR(A2-C)	GAGGAGGACTTGTACACACACGATCTAAACAG
GC-cremut-REV(A2-C)	CTGTTTAGATCGTGTGTGTACAAGTCCTCCTC
GC-cremut-FOR(A3-C)	GAGGAGGACTTGTACAACCACGATCTAAACAG
GC-cremut-REV(A3-C)	CTGTTTAGATCGTGGTTGTACAAGTCCTCCTC
GC-cremut-FOR(A1A2-C)	GAGGAGGACTTGTACCCACACGATCTAAACAG
GC-cremut-REV(A1A2-C)	CTGTTTAGATCGTGTGGGTACAAGTCCTCCTC
T7crefor	AATTCTAATACGACTCACTATAGGGTCGCTTGAGGAGGACTTGTACAAACA CGATCTAAACAGGTTTCCCCAACTGACCCG
T7crerev	CTAGCGGGTCAGTTGGGGAAACCTGTTTAGATCGTGTTTGTACAAGTCCTC CTCAAGCGACCCTATAGTGAGTCGTATTAG
01Kcremut FOR(A1C)	GAGGAGGACTTGTACCAACACGATCTATGCAG
01Kcremut-REV(A1C)	CTGCATAGATCGTGTTGGTACAAGTCCTCCTC
01Kcremut-FOR(A2C)	GAGGAGGACTTGTACACACACGATCTATGCAG
01Kcremut-REV(A2C)	CTGCATAGATCGTGTGTGTACAAGTCCTCCTC
01Kcremut-FOR(A3C)	GAGGAGGACTTGTACAACCACGATCTATGCAG
01Kcremut-REV(A3C)	CTGCATAGATCGTGGTTGTACAAGTCCTCCTC
F-O1KcreDEL	GATTGTACTGAGAGTGCACCATATCGACGC
R-O1KcreDEL	GTTTCACAGTAAAGCTGCCGTGCTGGGGTT
F-O1KcreDEL-overlap	TTGAGGAGGACTTGTACCACGATCTATGCAGGTTTC
R-O1KcreDEL-overlap	GAAACCTGCATAGATCGTGGTACAAGTCCTCCTCAA

within the genome of FMDV. This element is about 55 nt in length and includes a conserved AAACA sequence, but in contrast to all other picornavirus *cre* structures, it is located within the 5′ untranslated region (5′ UTR) of the viral genome, immediately upstream of the internal ribosome entry site (IRES). This FMDV *cre* could be moved to the 3′ UTR while retaining activity. A role for this FMDV sequence in the uridylylation of FMDV VPg (3B) has not been reported but is assumed. The identification of a *cre* within the 5′ UTR of FMDV explained the phenotype of a temperature-sensitive (*ts*) mutant (*ts*303) of FMDV which is RNA replication defective under the nonpermissive conditions (39). Unexpectedly, the *ts* lesion in this virus was located within the 5′ UTR, and this mutation is now known to reduce the stability of the stem of the FMDV *cre* (39). A revertant of the *ts* mutant had a second mutation that restored the stability of this structure. A remarkable feature of this mutant is that its defect in replication could be complemented in *trans*. Thus, it appears that the FMDV *cre* can function in *trans*, and it was suggested (39) that a better name for this element may be a 3*B-u*ridylylation *s*ite (*bus*). It is interesting that the role of the PV *cre* in the in vitro uridylylation of the PV VPg can also be performed in *trans* (17).

There are important differences between the properties of FMDV compared to PV with respect to virus replication. For example, FMDV uniquely expresses 3 distinct copies of the viral protein 3B (3B1, 3B2, and 3B3, or VPg1-3) as the primer for RNA replication, this feature is conserved in all strains of FMDV. Each of these different peptides has been shown to be used during virus replication and to be linked to genomic RNA (20). Deletion of the individual copies of VPg has a deleterious effect on RNA replication (9). In particular, deletion of the 3B3 coding sequence resulted in a nonviable virus, but this defect was attributed to impaired proteolytic processing of the polyprotein. In addition, a key feature of PV RNA replication is the role of the cloverleaf structure (about 80 nt) located at the 5′ terminus of the genome (2), but this feature is absent from FMDV RNA. Instead, the viral RNA has a 5′-terminal S-fragment (about 360 nt) that is predicted to form a large hairpin structure (6, 8). Furthermore, whereas PV replication is extremely sensitive to the action of brefeldin A (an agent that modifies intracellular Golgi membranes), the replication of FMDV is rather insensitive to this agent (25, 30), and this observation is suggestive of a different site of replication within the cytoplasm of the cell. It is therefore apparent that results obtained for PV cannot be assumed to be applicable to FMDV; hence, both the unique characteristics and economic importance of FMDV make it worthy of study.

We have now determined the FMDV components required for the uridylylation of each of the distinct FMDV 3B peptides by the FMDV $3D^{pol}$ in vitro.

MATERIALS AND METHODS

Construction of plasmids. The full-length FMDV infectious cDNA clone (pT7S3) of the O1Kaufbeuren strain (7) was used as the template for PCR amplification of specific FMDV coding sequences.

(i) pQE30/$3D^{pol}$. The coding sequence of the FMDV $3D^{pol}$ was amplified in a PCR with primers 3DFORBGL and 3DREVSPH, which contain BglII and SphI restriction sites, respectively (Table 1), using *Pfu* DNA polymerase. The product was ligated into the pT7blue vector (Novagen) to produce pT7/$3D^{pol}$. From this plasmid, the BglII-SphI fragment was excised and ligated into the bacterial

expression vector pQE30 (QIAGEN) previously digested with BamHI and SphI to produce pQE30/3D^{pol}. The vector adds an N-terminal His tag to the 3D^{pol} coding sequence.

(ii) pQE30/3CD^{pro}(C163G). The coding sequence for FMDV 3CD^{pro} was amplified in a PCR using oligonucleotides 3CFORBGL and 3DREVSPH (Table 1). The product was ligated into pT7blue (Novagen) to produce pT7/3CD^{pro}. This plasmid was used as a template for mutagenesis (using the QuikChange system [Stratagene] with primers C163FOR and C163REV) to change the codon within the 3C sequence corresponding to cysteine 163 to a glycine codon. The resulting plasmid was digested with BglII and SphI, and the fragment was ligated into BamHI-SphI-digested pQE30 to produce pQE30/3CD^{pro}(C163G). This plasmid encodes His-tagged 3CD in which the 3C protease activity is blocked.

(iii) pUb-3D^{pol}. To produce an unmodified FMDV 3D^{pol}, the system described by Gohara et al. (14) was employed. This entails the coexpression of a ubiquitin-tagged FMDV 3D^{pol} fusion protein with the ubiquitin (Ub) protease Ubp2. The coding sequence of the FMDV 3D^{pol} was amplified in a PCR with primers Ub3DpolSacII and Ub3DpolBglII (Table 1). The fragment (ca. 1,430 bp) was ligated into pT7blue (Novagen). Modification of an internal SacII site within the FMDV 3D^{pol} sequence was performed using the QuikChange mutagenesis kit (Stratagene) with the oligonucleotides SacIImutFor and SacIImutRev (Table 1) and verified by sequencing; this modification preserves the native amino acid sequence. The modified 3D^{pol} sequence was excised with SacII and BglII and ligated into a SacII- and BamHI-digested pET26b-Ub vector (kindly provided by Craig Cameron) (14) to produce pUb-3D^{pol}.

(iv) pGC-cre (wild-type [wt] and mutant forms). The plasmid pGC was a gift from Graeme Conn (University of Manchester) and contains the hepatitis D virus δ ribozyme cDNA (40). Oligonucleotides T7crefor and T7crerev (Table 1) corresponding to the FMDV OVI *cre*/*bus* (39) and preceded by a T7 promoter were annealed and ligated into this vector upstream of the ribozyme between the EcoRI and NheI sites to produce pGC-*cre*. This plasmid can be used to produce, from a T7 promoter, RNA transcripts that correspond to the FMDV *cre*/*bus*. The plasmid was modified using mutagenic primers (GC-cremut series) (Table 1) and a QuikChange mutagenesis kit (Stratagene) to construct plasmids which can be transcribed to produce mutant transcripts with A-to-C substitutions at positions 1 to 3 within the conserved AAACA motif.

(v) pT7S3 mutants. Modifications to the *cre*/*bus* sequence within the context of the full-length FMDV O1Kaufbeuren RNA were performed by modifying the plasmid pT7S3 that can be transcribed to produce infectious RNA transcripts (7). This plasmid was digested with SpeI and NotI, and the 3,068-bp fragment was ligated into similarly digested pGEM-5Z vector (Promega) to produce pGEM-5Z/SN, which was used as a template for modification of each of the first 3 A residues of the AAACA motif within the *cre*/*bus* using QuikChange site mutagenesis as described above with the O1Kcremut primers listed in Table 1. The modified fragments containing the required mutations were released from pGEM-5Z/SN derivatives and reconstructed back into the pT7S3 backbone. The respective mutations in the full-length cDNA were verified by sequencing.

To achieve a deletion of the AAA sequence from the AAACA motif, an overlap PCR was performed using the O1KcreDel primers (Table 1), with pT7S3 as the initial template. The final product (1,250 bp) was digested with SpeI and XbaI to generate a 743-bp fragment which was ligated into the similarly digested pT7S3 backbone to produce pT7S3creDel. The presence of the required mutation in the *cre*/*bus* region in this plasmid was verified by sequencing.

Production of wild-type and mutant FMDV *cre*/*bus* transcripts. The plasmid pGC-*cre* (wt) and the various mutants were used as templates for production of RNA transcripts. Plasmid DNAs were linearized with NheI and purified by phenol extraction and ethanol precipitation, and RNA was produced using a MEGAscript high-yield transcription kit according to the manufacturer's instructions (Ambion). The products were treated with DNase I and purified using urea-polyacrylamide (12%) gel electrophoresis. The transcripts were detected by UV shadowing, eluted in EDTA (1 mM) and sodium dodecyl sulfate (SDS, 0.5%), and isolated by phenol extraction and ethanol precipitation. Analysis of the RNA transcripts, using 8% polyacrylamide–urea gels, showed single bands (data not shown). RNA transcripts were stored at −70°C.

Production of full-length wild-type and mutant FMDV RNA transcripts. The plasmid pT7S3 and its derivatives were linearized downstream of the poly(A) tail at a unique HpaI site and used for the production of full-length RNA transcripts as described above. The transcripts were purified by phenol extraction and ethanol precipitation and quantified using a spectrophotometer. Truncated transcripts lacking the poly(A) tail or the entire coding sequence were generated in the same way but using templates that had been linearized with EcoNI or XbaI, respectively, as indicated in the figure legends.

Expression and purification of His-tagged FMDV proteins. To express each His-tagged protein, the appropriate plasmid was transformed into *Escherichia coli* strain M15 and grown in NZYCM medium containing kanamycin (25 μg/ml) and ampicillin (50 μg/ml) at 37°C to an A_{600} of 1.0. The cultures were cooled to 28°C, and expression was induced with isopropyl-1-thio-β-D-galactopyranoside (IPTG) (500 μM for His-3D^{pol} or 100 μM for His-3CD). The cells were harvested at 6,000 rpm for 15 min, washed once in TE (10 mM Tris, 1 mM EDTA), and centrifuged again. The cell paste was weighed and stored at −70°C. Frozen cells were thawed and resuspended in lysis buffer (potassium phosphate [50 mM, pH 8.0], sodium chloride [500 mM], glycerol [20%], β-mercaptoethanol [10 mM], pepstatin A [2 μg/ml], leupeptin [2.8 μg/ml], and NP-40 [0.1%]) using 5 ml/g of cells. The samples were frozen/thawed again and lysed by sonication. Phenylmethylsulfonyl fluoride (1 mM) was added, and nucleic acids were precipitated by the addition of polyethyleneimine to a final level of 0.25% (vol/vol) over a 30-min period with constant stirring. The extract was centrifuged (30 min at 15,000 rpm), and ammonium sulfate was added to the supernatant to 40% saturation. The precipitated material was harvested (30 min at 15,000 rpm), resuspended in buffer A (Tris [50 mM, pH 8.0], 20% glycerol, sodium chloride [50 mM], β-mercaptoethanol [10 mM], and 0.1% NP-40) and dialyzed overnight against the same buffer. The sample was loaded onto a 15-ml phosphocellulose column (Whatman) at a flow rate of 0.5 ml/min. The column was washed with buffer A, and protein was eluted using a linear gradient (5 column volumes) from 50 mM to 1 M NaCl in buffer A. Peak fractions were pooled and dialyzed against buffer A for 2 h and loaded onto a Hi-Trap His column (1 ml; Amersham Bioscience). The column was washed twice with wash buffer B (sodium phosphate [50 mM, pH 8.0], NaCl [500 mM], and imidazole [20 mM]), and the His-tagged protein was eluted with buffer B (2 ml) with added imidazole (500 mM). The eluted His-3D^{pol} and His-3CD samples were dialyzed against buffer A containing 50 mM and 500 mM NaCl, respectively. Protein samples were analyzed by SDS-polyacrylamide gel electrophoresis (PAGE) (21) and immunoblotting using anti-FMDV 3D antibodies (3B9) (a kind gift of E. Brocchi, Brescia, Italy) and chemiluminescence reagents (Amersham Bioscience).

Production of unmodified FMDV 3D^{pol}. Expression and purification of the untagged FMDV 3D^{pol} was achieved using a protocol essentially as described previously (14). Briefly, BL21(DE3) cells containing both the pUb-3Dpol and pCG1 plasmids (the latter expresses the Ubp2 protease) were grown overnight in NZCYM media with kanamycin (25 μg/ml), chloramphenicol (20 μg/ml), and 0.4% glucose at 30°C. The culture was used to inoculate fresh media and grown to an optical density at 600 nm of 1.0 at 37°C. The cells were cooled to 28°C, IPTG (500 μM) was added, and the mixture was incubated for an additional 4 h at 28°C. Cells were extracted, and the proteins were concentrated as described above. Then after the phosphocellulose column, the sample was loaded onto a Q-Sepharose column (1 ml; Amersham Biosciences) at 0.2 ml/min. The column was washed with buffer A, and proteins were eluted with a linear gradient (5 column volumes) from 50 mM to 1.5 M NaCl in buffer A. Peak fractions were pooled and dialyzed for 2 h against buffer A. The dialyzed sample was loaded onto a 1-ml Hi-Trap heparin column (Amersham Biosciences), and the bound protein was eluted using 2 column volumes of buffer A with a linear gradient of 50 mM to 1.5 M NaCl. The peak fractions were pooled and dialyzed against buffer A with 50 mM NaCl.

Synthesis of synthetic peptides corresponding to 3B1, 3B2, and 3B3. Synthetic peptides corresponding to the individual FMDV 3B1, 3B2, and 3B3 peptides and a modified version containing a single-amino-acid substitution (Y to F) were produced by Lawrence Hunt (Institute for Animal Health, Compton Lab) and purified by high-performance liquid chromatography.

Estimation of protein concentrations. Protein concentrations were determined using the following molar extinction coefficients: 1,280 M^{-1} cm^{-1} for VPg1, VPg2, and VPg3; 51,850 M^{-1} cm^{-1} for 3D^{pol}; 61,170 M^{-1} cm^{-1} for 3CD. These values were determined using the protein parameters tool on the ExPASy website. The absorbance values were measured at 280 nm in 6 M guanidine–HCl, pH 6.5.

In vitro RNA synthesis assays. Poly(U) polymerase assays were performed essentially as described previously (14) in HEPES (50 mM, pH 7.5), 2-mercaptoethanol (10 mM), $MgCl_2$ or $MnCl_2$ (as indicated, 5 mM), $ZnCl_2$ (60 μM), UTP (500 μM), [α-^{32}P]UTP (0.2 μCi/μl), dT_{15} (1.8 μM)-poly(rA)$_{500}$ (0.15 μM) primer-template, and 3D^{pol} (1 μM) using a total volume of 20 μl. Samples were prewarmed to 30°C, and reactions were initiated by the addition of 3D^{pol}. Mixtures were then incubated for 5 min, and assays were stopped by the addition of EDTA (final concentration, 100 mM). Aliquots (10 μl) were spotted onto DE81 filter paper disks which were then washed three times for 5 min in 5% dibasic sodium phosphate and rinsed in absolute ethanol. Bound radioactivity was quantified by liquid scintillation counting, and the rate of UMP incorporation was calculated.

In vitro uridylylation assay. The synthesis of VPgpU(pU) was measured using an assay similar to that described previously (16, 33). The reaction mixture (total

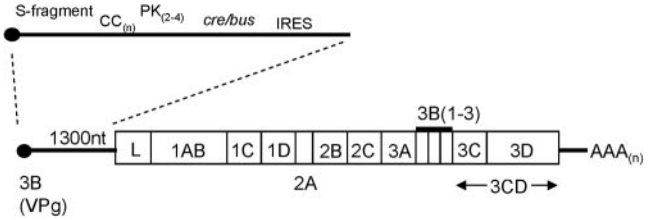

FIG. 1. Genome organization of FMDV. The features of the 5′ UTR and the coding sequences used in this study are illustrated. The presence of three separate 3B peptide sequences and the *cre*/*bus* upstream of the IRES within the 5′ UTR are indicated. Abbreviations: PK, pseudoknots; CCn, poly(C) tract.

volume, 20 μl) contained 50 mM HEPES (pH 7.5), glycerol (8%), $MgCl_2$ (2 mM), 3B/VPg (12.5 μM or as indicated in the figure legends), *cre*/*bus* RNA transcripts (1 μM or as indicated in the figure legends), [α-^{32}P]UTP (0.75 μCi; Amersham Bioscience), UTP (10 μM), His-3CD(C163G) (1 μM), and 3D^{pol} (1 μM). The final NaCl concentration in the reaction mixture (from the protein solutions) was kept at 6.25 mM. Mixtures were incubated for 30 min at 30°C, and reactions were stopped by the addition of Tris-Tricine loading dye (10 μl) and analyzed by Tris-Tricine sodium dodecyl sulfate-polyacrylamide gel electrophoresis with 14% polyacrylamide. Gels were dried without fixing and autoradiographed. The reaction products were quantitated with a PhosphorImager (Molecular Imager FX; Bio-Rad) to determine the level of [^{32}P]UMP incorporation. VPgpU(pU) refers to the sum of VPgpU and VPgpUpU. In some reaction mixtures, the *cre*/*bus* RNA transcripts were replaced by other RNA transcripts as described in the figure legends. Uridylylation assays using poly(A) as the template were performed as described previously (34).

PV uridylylation reaction components. The PV (type 3) 3D^{pol} was expressed as a Ub-tagged fusion protein as described above for the FMDV 3D^{pol}, and the untagged product that was generated was purified using phosphocellulose and Q-Sepharose chromatography (I. G. Goodfellow, unpublished data). The PV 3 *cre*, PV VPg, and 3CD have been described previously (16).

RESULTS

Requirements for the uridylylation of FMDV 3B. Studies on the replication of PV and HRV RNA have established the requirements for in vitro uridylylation of 3B (VPg) to be 3B, 3D^{pol}, 3CD, RNA transcripts containing the *cre* plus UTP, and divalent metal ions, either Mn^{2+} or Mg^{2+} (12, 13, 34, 35). To establish this assay for the FMDV components, it was necessary to generate these reagents (Fig. 1).

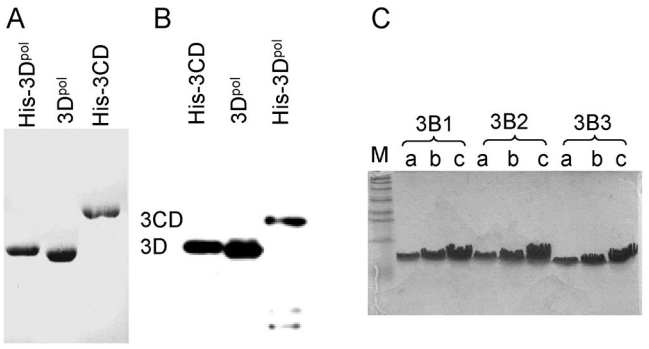

FIG. 2. Gel analysis of FMDV 3D^{pol}, His-3D, 3CD, and 3B1 to 3. Purified recombinant His-tagged 3D (termed His-3D), His-tagged 3CD(C163G) (termed His-3CD), and the untagged 3D (3D^{pol}) were analyzed by SDS-PAGE and either stained directly with Coomassie blue (A) or transferred to an Immobilon membrane and detected using an anti-3D monoclonal antibody (kindly provided by E. Brocchi) with peroxidase-labeled goat anti-mouse immunoglobulin and chemiluminescence reagents (B). (C) Synthetic peptides (10 nmol [lanes a], 20 nmol [lanes b], or 30 nmol [lanes c]) corresponding to 3B1, 3B2, and 3B3 were analyzed on Tris-Tricine gels (16.5% acrylamide) and stained with Coomassie blue. Lane M contains a molecular weight marker (175,000 to 6,000; New England Biolabs).

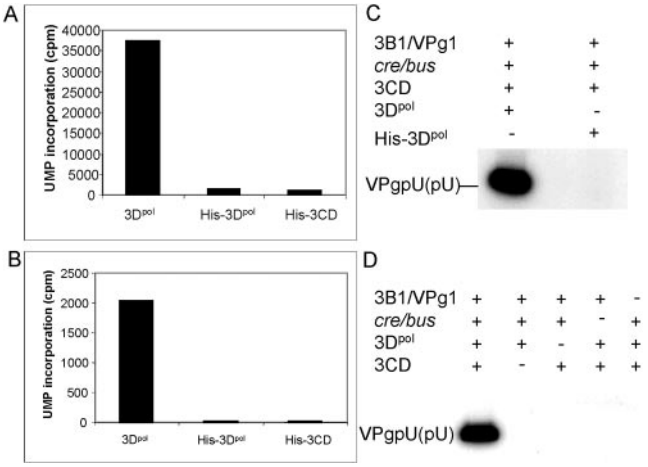

FIG. 3. In vitro RNA synthesis and 3B1 uridylylation by FMDV 3D^{pol}. (A and B) In vitro RNA synthesis assays using a poly(rA)$_{500}$ (0.15 μM) template and dT_{15} (1.8 μM) primer were performed with the His-tagged 3D^{pol} (1 μM), His-tagged 3CD (1 μM), and untagged 3D^{pol} (1 μM) as indicated in the presence of Mn^{2+} (5 mM) (A) or Mg^{2+} (5 mM) (B). The incorporation of [^{32}P]UMP (from UTP) was measured at 5 min when the assays were within a linear range, and the reactions for panels A and B were performed in parallel. (C) In vitro 3B uridylylation assays were performed using the 3B1 peptide (12.5 μM) with [α-^{32}P]UTP in the presence of Mg^{2+} (2 mM) with His-tagged 3CD (1 μM), the *cre*/*bus* RNA transcripts (1 μM), and either the untagged 3D^{pol} or the His-tagged 3D^{pol}, as indicated. The uridylylated 3B1/VPg1 product, termed VPgpU(pU), is indicated. (D) In vitro 3B uridylylation assays were performed as described for panel C, and the individual components of the uridylylation reaction were separately omitted, as indicated. +, present; −, absent.

The coding region for FMDV 3D^{pol} was amplified using a PCR and inserted into the bacterial expression vector pQE30 (QIAGEN). An N-terminal His-tagged form of 3D^{pol} was efficiently expressed from this vector in *E. coli* M15 and purified using Ni-nitrilotriacetic acid resin to near homogeneity as judged by Coomassie blue staining and immunoblotting using anti-3D antibodies (Fig. 2A and B). Similarly, cDNA encoding the FMDV 3CD precursor protein was amplified by PCR. The catalytic activity of the 3C protease was blocked by modification of the Cys codon (TGC) at residue 163 to a glycine (GGC) codon within the 3C sequence (see reference 18). This modification was verified by DNA sequencing, and the mutant 3CD coding sequence was inserted into pQE30 as described above. The His-tagged 3CD(C163G) was also efficiently expressed in *E. coli* M15 and purified to near homogeneity (Fig. 2A and B). As expected, the 3CD migrated more slowly than the 3D^{pol}, confirming that the modification of the 3C sequence blocked its proteolytic activity. When tested within an in vitro RNA polymerase assay (14), using poly(A) as template, the His-tagged 3D^{pol} and the His-tagged 3CD(C163G) exhibited little or no RNA polymerase activity in the presence of Mg^{2+} but both proteins displayed significant activity in the presence of Mn^{2+} (Fig. 3A and B). This result should be compared with the complete lack of RNA polymerase activity exhibited by the PV 3CD (see reference 38); indeed, the complete inactivity of

the PV 3CD was confirmed in our assays (data not shown). There is conflicting evidence about the ability of different picornavirus $3D^{pol}$ molecules with some form of N-terminal extension to function as an RNA polymerase. The PV $3D^{pol}$ poorly tolerates even a single extra amino acid (14), whereas the $3D^{pol}$ from HRV-2 within a glutathione *S*-transferase–$3D^{pol}$ fusion protein exhibited RNA polymerase activity similar to that of the untagged $3D^{pol}$ (12, 13).

The His-tagged $3D^{pol}$ with His-tagged 3CD was tested in an in vitro uridylylation assay using RNA transcripts corresponding to the FMDV *cre*/*bus* with the FMDV 3B peptides, which were prepared as synthetic peptides and appeared homogeneous, as judged by Coomassie blue staining of Tris-Tricine gels (Fig. 2C), but no uridylylation of the peptides was observed (Fig. 3C).

To express the FMDV $3D^{pol}$ without any additional sequences, the $3D^{pol}$ cDNA was amplified using a PCR, modified to remove an internal SacII site, and inserted into the vector pET26-Ub (14) to generate pUb3D^{pol}. This plasmid efficiently expressed a ubiquitin-tagged FMDV $3D^{pol}$ in *E. coli*, and when coexpressed with the ubiquitin-specific protease Ubp2, by cotransformation of *E. coli* BL21(DE3) with pUb3D^{pol} and pCG1, cleavage occurred efficiently to liberate the untagged FMDV $3D^{pol}$ (data not shown). The unmodified FMDV $3D^{pol}$ was then purified to near homogeneity using phosphocellulose, anion exchange, and heparin chromatography (Fig. 2A). This untagged FMDV $3D^{pol}$ migrated slightly faster on SDS-PAGE than the His-tagged $3D^{pol}$ (Fig. 2A and B). The native FMDV $3D^{pol}$ exhibited high RNA polymerase activity using poly(A) as a template (Fig. 3A and B). This activity was also markedly greater in the presence of Mn^{2+} rather than Mg^{2+} (compare Fig. 3A and B). It is noteworthy that the incorporation of UMP by the unmodified $3D^{pol}$ in the presence of Mg^{2+} is comparable to that achieved by the His-tagged $3D^{pol}$ and the His-3CD in the presence of Mn^{2+}. The specific activity of the unmodified FMDV $3D^{pol}$ in the presence of Mn^{2+} was 247 pmol/min/μg, whereas in the presence of Mg^{2+}, it was 15 pmol/min/μg.

Reactions were then performed to analyze the ability of the untagged FMDV $3D^{pol}$ to uridylylate the FMDV 3B1 peptide using [α-^{32}P]UTP, an RNA transcript (56 nt) corresponding to the FMDV *cre*/*bus*, His-tagged 3CD, and divalent metal ions. In contrast to the result using the His-tagged $3D^{pol}$, it was found that the production of [^{32}P]-labeled uridylylated 3B1 was observed (Fig. 3C). The requirements for the different components of this reaction were then determined; it was found that omission of the short RNA transcript, or His-3CD (C163G), or $3D^{pol}$ totally abrogated uridylylation of 3B1 (Fig. 3D). A very similar pattern of results was observed in the presence of either Mg^{2+} or Mn^{2+} ions (data not shown, see below).

Role of the *cre*/*bus* in uridylylation of FMDV 3B peptides. To study the effects of mutations in the loop region of the FMDV *cre*/*bus* in the VPg uridylylation assay, mutant *cre*/*bus* plasmids were generated. The first A residue in the conserved $A^1A^2A^3CA$ motif from the PV *cre* acts as the template for the addition of two U residues to the VPg peptide primer; the second and third A residues modulate this process (36). Mutations (A to C) were introduced in the FMDV *cre*/*bus* at the A^1, A^2, and A^3 positions individually, and a fourth mutant was made with mutations at both the A^1 and A^2 positions. Short RNA transcripts were prepared from each of these plasmids,

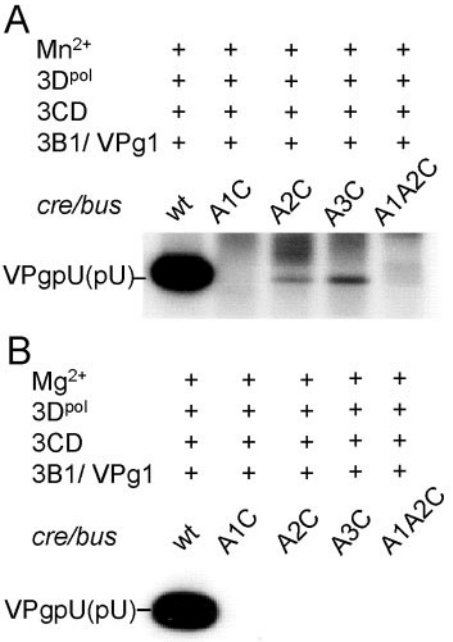

FIG. 4. Critical role of the AAACA motif within the FMDV *cre*/*bus* for in vitro uridylylation of FMDV 3B1. In vitro uridylylation assays using the FMDV 3B1 peptide were performed using wt or mutant FMDV *cre*/*bus* RNA transcripts as indicated in the presence of Mn^{2+} (A) or Mg^{2+} (B) with FMDV $3D^{pol}$ and His-3CD. Reaction mixtures were incubated at 30°C for 30 min. +, present.

and their ability to support the uridylylation of FMDV 3B1 was tested in the presence of Mn^{2+} or Mg^{2+} ions (Fig. 4A and B). In the presence of each of the divalent metal ions, the wt *cre*/*bus* transcript supported very efficient uridylylation of 3B1. However, substitution of A^1 alone or A^1 and A^2 together in the *cre*/*bus* transcripts completely blocked the reaction. In the presence of Mg^{2+} ions (Fig. 4B), the A^2 and A^3 point mutants were also inactive, but in the presence of Mn^{2+} ions, very low level uridylylation of the 3B1 peptide was also observed using the A^2 and A^3 mutant transcripts as templates (Fig. 4A).

Uridylylation of the three different FMDV 3B peptides. Uniquely, FMDV encodes and uses three distinct forms of 3B (VPg) which differ in size and sequence (Fig. 5A). Each of the different forms of FMDV 3B has been found to be associated with genomic RNA, and hence, all must be functional (20). The activity of the three different peptides in the in vitro uridylylation assay was compared (Fig. 5B and C). It was apparent that each of the 3B peptides could be uridylylated in vitro by the untagged $3D^{pol}$ in the presence of the *cre*/*bus* transcripts and His-3CD. However, it appeared that 3B3 was a better substrate in this assay than 3B2, which in turn was also better than 3B1. It was also apparent that the uridylylation reaction occurred with similar efficiency in the presence of Mn^{2+} or Mg^{2+} (Fig. 5B and C) and the relative efficiency of uridylylation of the different 3B peptides was the same with each divalent metal ion. Each of the 3B peptides migrated slightly differently on the Tris-Tricine gels (Fig. 5B). Thus, although 3B1 is one amino acid shorter than 3B2 and 3B3 (Fig. 5A), it migrated at an intermediate position and 3B3 migrated the fastest. To confirm the differences in efficiency of uridylylation, we determined the rate of UMP incorporation in a time course

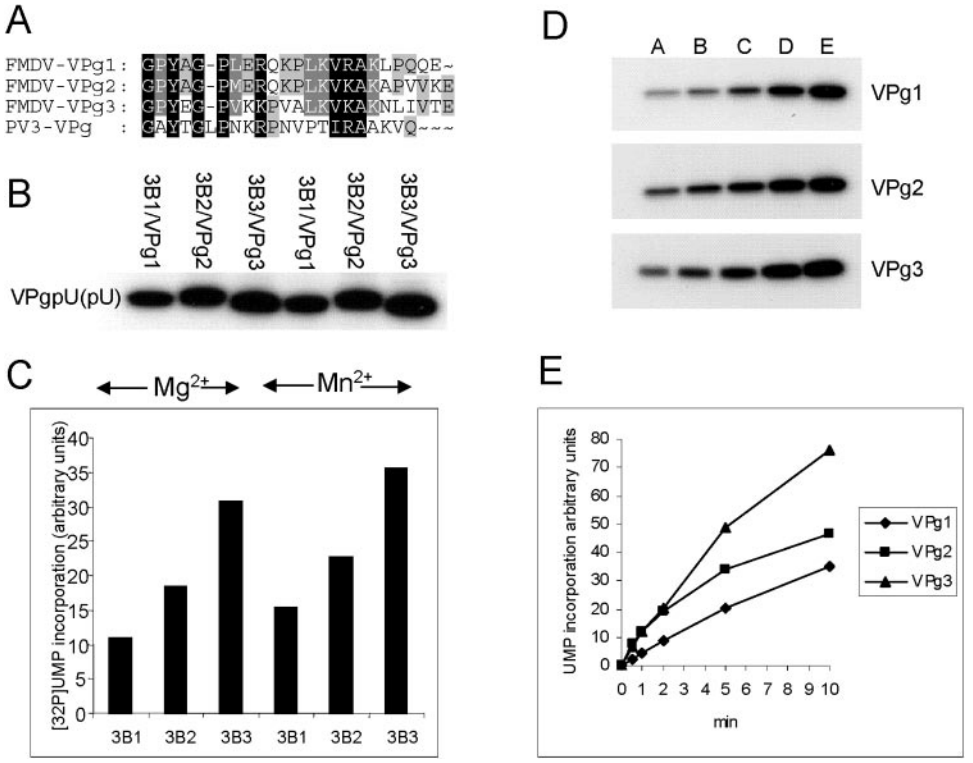

FIG. 5. In vitro uridylylation of all three FMDV 3B peptides. (A) Comparison of VPg sequences from FMDV (O1Kaufbeuren) and PV (type 3). The conserved Tyr (Y) (residue 3) is the site of uridylylation. (B) In vitro uridylylation assays were performed in the presence of purified FMDV components $3D^{pol}$ (1 μM), His-3CD (1 μM), *cre*/*bus* RNA transcripts (1 μM), and either Mn^{2+} (2 mM) or Mg^{2+} (2 mM), as indicated, using each of the FMDV 3B peptides (12.5 μM). Products were analyzed on Tris-Tricine gels. (C) Incorporation of [α-^{32}P]UMP into VPgpU(pU) was quantitated for each peptide using a phosphorimager. (D) The time course of uridylylation of VPg1, VPg2, and VPg3 was determined in parallel. Reactions were performed as described for panel B with Mg^{2+} (2 mM), and each VPg peptide was used at 1 μM. The time points were 30 s (A), 1 min (B), 2 min (C), 5 min (D), and 10 min (E). (E) The incorporation of UMP in the reactions shown in panel D was quantified using a phosphorimager.

assay for each VPg in parallel (Fig. 5D and E). Consistent with the results shown in Fig. 5B and C, the rate of VPg3 (3B3) uridylylation was the fastest, while that for VPg1 (3B1) was the slowest and VPg2 (3B2) was intermediate.

Specificity of 3B (VPg) recognition in the uridylylation assay. The linkage of VPg (3B) to RNA occurs through the hydroxyl group on a Tyr residue. To confirm that the uridylylation reaction observed with the FMDV components was dependent on the presence of the Tyr residue, a variant of the 3B3 peptide was synthesized in which the Tyr was replaced by a Phe residue (which lacks the hydroxyl group). This peptide was inactive in the uridylylation reaction, as anticipated (Fig. 6A). The ability of the PV VPg to be recognized by the FMDV components was also analyzed; this peptide is significantly different in sequence from each of the FMDV VPgs (Fig. 5A). Surprisingly, the PV VPg was very efficiently uridylylated using the FMDV components (Fig. 6B). In contrast, use of the PV uridylylation assay components showed high specificity for the PV VPg and no uridylylation of FMDV VPgs was observed (Fig. 6C). Thus, the basis of 3B/VPg recognition by the FMDV components is clearly complex.

Context of RNA template determines uridylylation efficiency. In the experiments described above, a small RNA transcript including the FMDV *cre*/*bus* sequence was used as the template in the uridylylation assay. Clearly, this element normally has to function in the context of a full-length (FL) viral RNA, and second, it is possible that uridylylation of 3B/VPg may also occur on the poly(A) tail at the 3′ terminus of the viral RNA. To investigate this, uridylylation reactions were performed using $3D^{pol}$, His-3CD, 3B3, and RNA transcripts corresponding to the wt FL RNA. Efficient uridylylation was observed in the presence of all of these components, but omission of any one of them blocked the reaction (Fig. 7A). A very low level of product was observed in the absence of His-3CD alone, but this was over 100-fold less abundant [note, no production of VPgpU(pU) has been observed in the absence of 3CD using the 3B3 peptide with the *cre*/*bus* template]. When mutant FL transcripts were used in which the *cre*/*bus* sequence was modified or deleted, it was found that modification of the A^1 position within the AAACA motif of the *cre*/*bus* or deletion of A^1, A^2, and A^3 (as in the creDel transcript) completely blocked activity but a weak signal (about 1% of that of the wt) was observed in the presence of Mg^{2+} (and Mn^{2+}) (data not shown) when A^2 or A^3 alone was modified (Fig. 7B). The overall pattern of these results closely matches those observed with the short *cre*/*bus* transcripts (Fig. 4), but it is apparent that the FL transcripts with A^2 or A^3 modified were more active than the short *cre*/*bus* transcripts containing these modifications. In the absence of a functional AAACA motif within the FL RNA, no uridylylation of the 3B3 occurred, indicating that

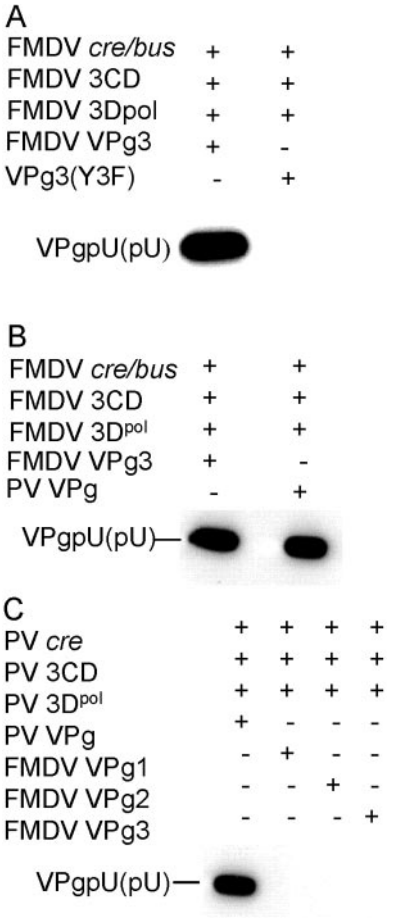

FIG. 6. Specificity of the VPg uridylylation reaction. (A) In vitro uridylylation assays were performed with [α-^{32}P]UTP using the FMDV *cre*/*bus* RNA transcript in the presence of Mg^{2+} with FMDV 3D^{pol} and His-3CD with either the FMDV VPg3 (3B3) peptide or the VPg3 (Y3F) peptide, as indicated. The latter peptide has the Tyr (Y) residue replaced by a Phe (F) residue. (B) In vitro uridylylation assays were performed as described for panel A using either FMDV VPg3 or the PV (type 3) VPg, as indicated. (C) In vitro uridylylation reactions were performed using PV components with either the PV VPg or each of the FMDV VPg peptides, as indicated. +, present; −, absent.

the poly(A) tail was not functional in this assay (Fig. 7B). RNA transcripts corresponding to the FMDV 5′ UTR down to an XbaI site (about 40 nt downstream from the *cre*/*bus*) were also very efficient (about 50% compared to the FL RNA) as templates for the uridylylation of 3B3. Indeed, since within this assay the various RNA transcripts were used at the same molar concentration, it is apparent that the full-length RNA and the truncated 5′ UTR were significantly better templates than the *cre*/*bus* element alone (Fig. 7B). In previous studies (34), it has been shown that the PV 3D^{pol} can generate VPgpU(pU) using a poly(A) template in the presence of Mn^{2+} and this occurs most efficiently in the absence of 3CD. These results were reproduced using PV 3D^{pol} (Fig. 7C). However, in contrast, no significant uridylylation of FMDV VPg3 was observed using FMDV 3D^{pol} with a poly(A) template in the presence of Mg^{2+}, but a very weak signal was observed, on long exposure, in the presence of Mn^{2+} (Fig. 7C).

DISCUSSION

The studies performed here have shown that the formation of the FMDV VPgpU(pU), a primer for viral RNA synthesis, can be achieved with defined purified components. In addition to UTP (with divalent metal ions) and a FMDV 3B peptide, the reaction required RNA transcripts containing the *cre*/*bus*, the untagged 3D^{pol}, and the 3CD precursor. Each of the three distinct FMDV 3B peptides is an efficient substrate in this reaction, although the 3B3 showed the highest activity. Within the RNA, the AAACA motif within the *cre*/*bus* was shown to be critical for activity but poly(A) was essentially nonfunctional.

Previous studies have shown that modifications at the N terminus of PV 3D^{pol} have a deleterious effect on the activity of this protein (14, 38). Similarly, the coxsackie virus A21 is only active in an untagged form (13), whereas in contrast, the 3D^{pol} from HRV-2 displayed similar activity in an untagged form and as part of a glutathione *S*-transferase fusion protein. The activity of FMDV 3D^{pol} is clearly severely affected by the presence of the N-terminal His tag or by the presence of 3C sequences and has little or no activity in the presence of Mg^{2+} in the standard RNA polymerase assay. However, these proteins do display significant activity in the same assay with Mn^{2+}. Furthermore, with other templates, e.g., FL RNA, UMP incorporation into large products was observed from 3CD alone even in the presence of Mg^{2+} (Fig. 6A). The structure of the native FMDV 3D^{pol} has recently been published (10). It was found that the N-terminal region of the protein encircles the enzyme active site; hence, it is perhaps not very surprising that the presence of an N-terminal His tag perturbs the activity. It is clearly possible, however, for the presence of the tag to differentially affect the RNA polymerase activity (adding nucleotides to a growing oligonucleotide chain) compared to the uridylylation reaction (adding nucleotides to a peptide).

It is interesting that the 3B3 peptide was the most efficient substrate for uridylylation by the FMDV 3D^{pol} (Fig. 5B and C). Deletion of the individual 3B sequences from within FMDV RNA transcripts had shown that only the 3B3 sequence was essential for viability (9). However, this was attributed to a defect in proteolytic processing that was observed using in vitro translation reactions of the mutant transcripts. Since 3B3 also seems to be the most efficient substrate for in vitro uridylylation, it may be that the loss of this sequence may also have a deleterious effect on RNA replication, especially at the early stages of infection when the 3B peptides will be present at low levels. On the other hand, there was apparently little difference in the efficiency of virus rescue from the three different mutant transcripts in which two of the three 3B tyrosine (Y) residues were changed to phenylalanine (F). However, no sequence analysis of the rescued viruses was reported and each rescue was about 100-fold-less efficient than that of the wt (9).

The activity of the 3D^{pol} from PV and HRV-2 have both been shown to be much (10- to 100-fold) higher in the presence of Mn^{2+} than in the presence of Mg^{2+} (3, 13). The FMDV 3D^{pol} was also much more active (over 10-fold) with Mn^{2+} in the RNA polymerase assay. Within cells, the enzymes presumably function with Mg^{2+}. Studies suggest that the specificity of these RNA polymerases is relaxed in the presence of Mn^{2+}

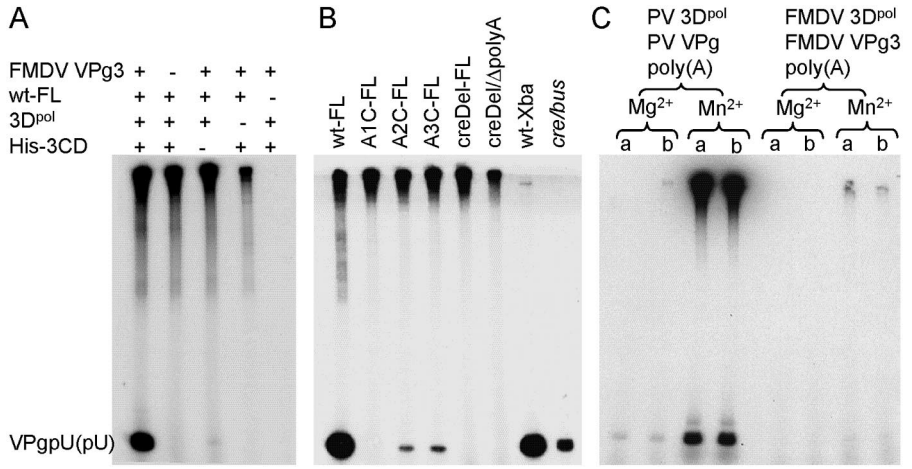

FIG. 7. The *cre*/*bus* is required for FMDV 3B3 uridylylation, and the context of this structure influences the efficiency of the reaction. (A) In vitro uridylylation assays were performed with [α-^{32}P]UTP in the presence of Mg^{2+} using the purified components 3B3 (12.5 μM), $3D^{pol}$ (1 μM), and His-3CD (1 μM) with FL wt FMDV RNA transcripts (25 nM), as indicated. (B) Uridylylation assays were performed with [α-^{32}P]UTP in the presence of Mg^{2+} using the purified components 3B3 (12.5 μM), $3D^{pol}$ (1 μM), and His-3CD (1 μM) using the different RNA transcripts indicated. Each transcript was used at the same concentration (25 nM). The FL RNA transcripts (wt or mutant, as indicated) were derived from HpaI-linearized plasmid DNA. Alternatively, truncated transcripts were produced following linearization with EcoNI, which removes the 3′ UTR plus the coding sequence for the C terminus of $3D^{pol}$, or linearization with XbaI, which removes all of the coding sequence plus most of the IRES but the transcript still includes the S fragment and the *cre*/*bus*. The uridylylated 3B3 [VPgpU(pU)] product is indicated. (C) Uridylylation reactions were performed using FMDV or PV components (as indicated, in the absence of 3CD) with poly(A) as the RNA template. Reactions were performed in the presence of Mg^{2+} or Mn^{2+} for 30 min (a) or 60 min (b), as shown. +, present; −, absent.

compared to Mg^{2+}, and this can lead to a higher level of misincorporation of nucleotides (3). The ability to use mutant forms of the short FMDV *cre*/*bus* transcripts in the uridylylation assay was also enhanced in the presence of Mn^{2+}, but there was little difference in the activity observed with each of these divalent metal ions when the wt *cre*/*bus* was used as a template with each of the 3B peptides (Fig. 5). These results closely match observations made with the PV $3D^{pol}$ (35; Goodfellow, unpublished).

Mutagenesis of the AAACA motif within the FMDV *cre*/*bus* showed that the A^1 nucleotide is critical for the uridylylation reaction (Fig. 4 and 7). This result is consistent with studies using a FMDV replicon containing modifications in this motif (24). Modification of the A^2 and A^3 nucleotides within this motif also greatly depressed viral RNA replication, and it is now shown that the in vitro uridylylation of 3B is also severely inhibited by these mutations in the *cre*/*bus*. Thus, the results on the requirements for the *cre*/*bus* in a FMDV replicon (24) closely match the in vitro studies on the uridylylation of 3B presented here. Furthermore, they are in accord with previous results on the role of the AAACA motif obtained in previous studies on the PV and HRV *cre* structures (35, 41). These results lead to the hypothesis that the first A nucleotide within this motif acts as the template for the addition of both the first and second U to 3B/VPg using a "slide-back" mechanism (36). It is interesting, however, that the FMDV *cre*/*bus* does not contain the consensus sequence derived from the PV and HRV *cre* sequences, ^{1}GXXXAAAXXXXXXA^{14}, or even the more relaxed version, RXXXAAAXXXXXXR. In the FMDV sequences studied, nt 14 is a C (see references 24, 36, and 39).

In a comparison between the template efficiency of the full-length RNA transcripts and the minimal *cre*/*bus* transcripts, it was apparent that the longer transcripts were significantly more efficient (Fig. 7B). This was also true for transcripts corresponding to just the 5′ terminal region of the genome (to just downstream of the *cre*/*bus*). These results may indicate that the stability of the *cre*/*bus* structure is greater when it is in the correct context or possibly that other sequences within the 5′ UTR (e.g., from the S fragment) may directly affect the efficiency of the uridylylation reaction. It is also interesting that the A^2 and A^3 mutants displayed activity (albeit at a low level) in the presence of Mg^{2+} ions within the context of the FL RNA transcripts but were completely inactive under these conditions using the short *cre*/*bus* transcripts. Hence, the specificity of the reaction is determined at least in part by the nature of the template.

There seemed to be no major role for the poly(A) tail in the in vitro uridylylation reaction, since there was a complete lack of uridylylation of 3B when the critical AAACA motif was modified or deleted (Fig. 7B). Furthermore, when poly(A) was used as the RNA template, no uridylylation of the FMDV 3B peptide was observed (Fig. 7C). This contrasts with earlier work which demonstrated the uridylylation of the PV VPg using a poly(A) template in the presence of Mn^{2+} (33, 34), a result which we have replicated (Fig. 7C). However, other recent studies have indicated that modification of the PV *cre* within full-length RNAs completely blocks VPg uridylylation within an in vitro replication system (29). Furthermore, when using purified components in the presence of Mg^{2+}, the formation of the PV VPgpU(pU) was dependent on the presence of the *cre* (16), whereas formation of VPg-poly(U) could occur on templates lacking this structure, e.g., poly(A) (Fig. 7C). Thus, it appears that under physiological conditions the formation of VPgpU(pU) by the FMDV $3D^{pol}$ requires the *cre*/*bus* and that the poly(A) tail does not support this reaction.

The uridylylation of the FMDV 3B peptides was completely

dependent on the presence of the His-tagged 3CD in addition to the *cre*/*bus* RNA and $3D^{pol}$. Studies on the PV system have found that the PV 3C alone can replace 3CD (31). The 3C must presumably interact with both the PV *cre* and $3D^{pol}$. There are significant differences between the properties of the PV 3C and 3CD. Both proteins are active proteases, but the PV 3CD is required for processing of the capsid precursor P1 (22), whereas in contrast, the FMDV 3C is able to achieve all capsid processing by itself (37). Hence, it will be interesting to determine whether the role of the FMDV 3CD in 3B uridylylation can also be replaced by 3C alone.

ACKNOWLEDGMENTS

A.N. gratefully acknowledges support from a Commonwealth Scholarship and from the Institute for Animal Health. I.G.G. acknowledges financial support from the Wellcome Trust.

We thank Lawrence Hunt (IAH, Compton) and Satya Parida (IAH, Pirbright) for the synthesis and provision of the FMDV 3B peptides. We also thank Graeme Conn (University of Manchester) and Craig Cameron (Penn State University) for plasmids and E. Brocchi (Brescia, Italy) for anti-$3D^{pol}$ antibodies.

REFERENCES

1. **Agol, V. I.** 2002. Picornavirus genome: an overview, p. 127–148. *In* B. L. Semler and E. Wimmer (ed.), Molecular biology of picornaviruses. ASM Press, Washington, D.C.
2. **Andino, R., G. E. Rieckhof, and D. Baltimore.** 1990. A functional ribonucleoprotein complex forms around the 5′ end of poliovirus RNA. Cell **63:** 369–380.
3. **Arnold, J. J., S. K. Ghosh, and C. E. Cameron.** 1999. Divalent cation modulation of primer, template, and nucleotide selection. J. Biol. Chem. **274:** 37060–37069.
4. **Belsham, G. J., and C. J. Bostock.** 1988. Studies on the infectivity of foot-and-mouth disease virus RNA using microinjection. J. Gen. Virol. **69:**265–274.
5. **Belsham, G. J., and E. Martinez-Salas.** 2004. Genome organization, translation and replication of foot-and-mouth disease virus RNA, p. 19–52. *In* F. Sobrono and E. Domingo (ed.), Foot and mouth disease: current perspectives. Horizon Bioscience, Norfolk, England.
6. **Clarke, B. E., A. L. Brown, K. M. Currey, S. E. Newton, D. J. Rowlands, and A. R. Carroll.** 1987. Potential secondary and tertiary structure in the genomic RNA of FMDV. Nucleic Acids Res. **15:**7067–7079.
7. **Ellard, F. M., J. Drew, W. E. Blakemore, D. I. Stuart, and A. M. King.** 1999. Evidence for the role of His-142 of protein 1C in the acid-induced disassembly of foot-and-mouth disease virus capsids. J. Gen. Virol. **80:**1911–1918.
8. **Escarmis, C., M. Toja, M. Medina, and E. Domingo.** 1992. Modifications of the 5′ untranslated region of foot-and-mouth disease virus after prolonged persistence in cell culture. Virus Res. **26:**113–125.
9. **Falk, M. M., F. Sobrino, and E. Beck.** 1992. VPg-gene amplification correlates with infective particle formation in foot-and-mouth-disease virus J. Virol. **66:**2251–2260.
10. **Ferrer-Orta, C., A. Arias, R. Perez-Luque, C. Escarmis, E. Domingo, and N. Verdaguer.** 2004. Structure of foot and mouth disease virus RNA-dependent RNA polymerase and its complex with a template-primer RNA. J. Biol. Chem. **279:**47212–47221.
11. **Gamarnik, A. V., and R. Andino.** 1998. Switch from translation to RNA replication in a positive-stranded RNA virus. Genes Dev. **12:**2293–2304.
12. **Gerber, K., E. Wimmer, and A. V. Paul.** 2001. Biochemical and genetic studies of the initiation of human rhinovirus 2 RNA replication: identification of a *cis*-replicating element in the coding sequence of 2Apro. J. Virol. **75:**10979–10990.
13. **Gerber, K., E. Wimmer, and A. V. Paul.** 2001. Biochemical and genetic studies of the initiation of human rhinovirus 2 RNA replication: Purification and enzymatic analysis of the RNA-dependent RNA polymerase $3D^{pol}$. J. Virol. **75:**10969–10978.
14. **Gohara, D. W., C. S. Ha, S. K. B. Ghosh, J. J. Arnold, T. J. Wisniewski, and C. E. Cameron.** 1999. Production of "authentic" poliovirus RNA-dependent RNA polymerase ($3D^{pol}$) by ubiquitin-protease-mediated cleavage in *Escherichia coli*. Protein Expr. Purif. **17:**128–138.
15. **Goodfellow, I. G., Y. Chaudhry, A. Richardson, J. Meredith, J. W. Almond, W. Barclay, and D. J. Evans.** 2000. Identification of a *cis*-acting replication element within the poliovirus coding region. J. Virol. **74:**4590–4600.
16. **Goodfellow, I. G., D. Kerrigan, and D. J. Evans.** 2003. Structure and function of the poliovirus *cis*-acting replication element (CRE). RNA. **9:**124–137.
17. **Goodfellow, I. G., C. Polacek, R. Andino, and D. J. Evans.** 2003. The poliovirus 2C *cis*-acting replication element-mediated uridylylation of VPg is not required for synthesis of negative-sense genomes. J. Gen. Virol. **84:**2359–2363.
18. **Grubman, M. J., M. Zellner, G. Bablanian, P. W. Mason, and M. E. Piccone.** 1995. Identification of the active-site residues of the 3C proteinase of foot-and-mouth disease virus. Virology **213:**581–589.
19. **Kaplan, G., and V. R. Racaniello.** 1988. Construction and characterization of poliovirus subgenomic replicons. J. Virol. **62:**1687–1696.
20. **King, A. M. Q., D. V. Sangar, T. J. R. Harris, and F. Brown.** 1980. Heterogeneity of the genome-linked protein of foot-and-mouth disease virus. J. Virol. **34:**627–634.
21. **Laemmli, U. K.** 1970. Cleavage of structural proteins during the assembly of the head of bacteriophage T4. Nature **227:**680–685.
22. **Leong, L. E. C., C. T. Cornell, and B. L. Semler.** 2002. Processing determinants and functions of cleavage products of picornavirus polyproteins, p. 187–197. *In* B. L. Semler and E. Wimmer (ed.), Molecular biology of picornaviruses. ASM Press, Washington, D.C.
23. **Lobert, P. E., N. Escriou, J. Ruelle, and T. Michiels.** 1999. A coding RNA sequence acts as a replication signal in cardioviruses. Proc. Natl. Acad. Sci. USA **96:**11560–11565.
24. **Mason, P. W., S. V. Bezborodova, and T. M. Henry.** 2002. Identification and characterization of a *cis*-acting replication element (*cre*) adjacent to the internal ribosome entry site of foot-and-mouth disease virus. J. Virol. **76:** 9686–9694.
25. **Maynell, L. A., K. Kirkegaard, and M. W. Klymkowsky.** 1992. Inhibition of poliovirus RNA synthesis by brefeldin A. J. Virol. **66:**1985–1994.
26. **McKnight, K. L., and S. M. Lemon.** 1996. Capsid coding sequence is required for efficient replication of human rhinovirus-14 RNA. J. Virol. **70:** 1941–1952.
27. **McKnight, K. L., and S. M. Lemon.** 1998. The rhinovirus type 14 genome contains an internally located RNA structure that is required for viral replication. RNA **4:**1569–1584.
28. **Morasco, B. J., N. Sharma, J. Parilla, and J. B. Flanegan.** 2003. Poliovirus *cre*(2C)-dependent synthesis of VPgpUpU is required for positive- but not negative-strand RNA synthesis. J. Virol. **77:**5136–5144.
29. **Murray, K. E., and D. J. Barton.** 2003. Poliovirus CRE-dependent VPg uridylylation is required for positive-strand RNA synthesis but not for negative-strand RNA synthesis. J. Virol. **77:**4739–4750.
30. **O'Donnell, V. K., J. M. Pacheco, T. M. Henry, and P. W. Mason.** 2001. Subcellular distribution of the foot-and-mouth disease virus 3A protein in cells infected with viruses encoding wild-type and bovine-attenuated forms of 3A. Virology. **287:**151–162.
31. **Pathak, H. B., S. K. B. Ghosh, A. W. Roberts, S. D. Sharma, J. D. Yoder, J. J. Arnold, D. W. Gohara, D. J. Barton, A. V. Paul, and C. E. Cameron.** 2002. Structure-function relationships of the RNA-dependent RNA polymerase from poliovirus ($3D^{pol}$). J. Biol. Chem. **277:**31551–31562.
32. **Paul, A. V.** 2002. Possible unifying mechanism of picornavirus genome replication, p. 227–246. *In* B. L. Semler and E. Wimmer (ed.), Molecular biology of picornaviruses. ASM Press, Washington, D.C.
33. **Paul, A. V., J. H. Boom, D. Filippov, and E. Wimmer.** 1998. Protein-primed RNA synthesis by purified poliovirus RNA polymerase. Nature **393:**280–284.
34. **Paul, A. V., E. Rieder, D. W. Kim, J. H. van Boom, and E. Wimmer.** 2000. Identification of an RNA hairpin in poliovirus RNA that serves as the primary template in the in vitro uridylylation of VPg. J. Virol. **74:**10359–10370.
35. **Paul, A. V., J. Peters, J. Mugavero, J. Yin, J. H. van Boom, and E. Wimmer.** 2003. Biochemical and genetic studies of the VPg uridylylation reaction catalyzed by the RNA polymerase of poliovirus. J. Virol. **77:**891–904.
36. **Paul, A. V., J. Yin, J. Mugavero, E. Rieder, Y. Liu, and E. Wimmer.** 2003. A "slide-back" mechanism for the initiation of protein-primed RNA synthesis by the RNA polymerase of poliovirus. J. Biol. Chem. **278:**43951–43960.
37. **Ryan, M., G. J. Belsham, and A. M. Q. King.** 1989. Specificity of enzyme-substrate interactions in foot-and-mouth disease virus polyprotein processing. Virology **173:**35–45.
38. **Thompson, A. A., and O. B. Peersen.** 2004. Structural basis for proteolysis-dependent activation of the poliovirus RNA-dependent RNA polymerase. EMBO J. **23:**3462–3471.
39. **Tiley, L., A. M. Q. King, and G. J. Belsham.** 2003. The foot-and-mouth disease virus cis-acting replication element (*cre*) can be complemented in *trans* within infected cells. J. Virol. **77:**2243–2246.
40. **Walker, S. C., J. M. Avis, and G. L. Conn.** 2003. General plasmids for producing RNA in vitro transcripts with homogeneous ends. Nucleic Acids Res. **31:**e82.
41. **Yang, Y., R. Rijnbrand, K. L. McKnight, E. Wimmer, A. Paul, A. Martin, and S. M. Lemon.** 2002. Sequence requirements for viral RNA replication and VPg uridylylation directed by the internal *cis*-acting replication element (*cre*) of human rhinovirus type 14. J. Virol. **76:**7485–7494.